Neural Network Approach for T-wave End Detection: A Comparison of Architectures

Alexander A. Suárez León[1], Danelia Matos Molina[1], Carlos R. Vázquez Seisdedos[1], Griet Goovaerts[2,3], Steven Vandeput[2,3], Sabine Van Huffel[2,3]

[1]Electrical Engineering Faculty, Universidad de Oriente, Santiago de Cuba, Cuba
[2]KU Leuven, Department of Electrical Engineering-ESAT, STADIUS Centre for Dynamical Systems, Signal Processing and Data Analytics, Belgium
[3]iMinds, Medical Information Technologies, Belgium

Abstract

In this paper, a new approach to the problem of detecting the end of the T wave (Te) on the electrocardiogram (ECG) using Multilayer Perceptron (MLP) neural networks is proposed and evaluated. The approach consists of a neural network acting as a regression function that estimates the Te location using the samples between two consecutive R peaks. The input vectors were taken using three dimensional reduction methods (Discrete Cosine Transform, DCT, Principal Component Analysis, PCA and resampling, RES) over a window of 100 samples. For training, Bayesian regularization has been used. A total of 1536 neural networks were trained. The results show that PCA and DCT are more feasible than RES as dimension reduction methods. Finally, a brief comparison with other algorithms proposed in the literature is included.

1. Introduction

The T-wave end point (Te) is in a slow transition zone of the electrocardiogram (ECG) signal, which is usually contaminated by noise and interference in ambulatory ECG. The standard deviation of the QT is small (<20 ms) for both healthy and pathological subjects. This requires a very high accuracy and precision for Te point detection algorithms.

There are several approaches proposed in the literature for the Te estimation. Vila *et al.* [1] presented a TU complex detection based on a mathematical model. Martínez *et al.* [2] used a quadratic spline wavelet at four dyadic scales for delineation. Other approaches are based on area computation [3, 4] and area-curve length indicator over the wavelet transform of the signal [5]. The partially collapsed Gibbs sampler was used in [6] and a mathematical model of a skewed Gaussian function combined with trapezium area method is described in [7].

This paper examines a new approach for Te detection using neural networks and methods for dimension reduction. Although the training of neural networks is a time-consuming operation, the advantage of the increased sensitivity is of greater importance than the added time delay, especially when dealing with Holter records which may have more than 80 000 beats. Moreover the training can be optimized through the selection of a small and representative dataset by the cardiologist, making this issue negligible.

2. Materials and methods

Detecting the Te point can be viewed as the problem of finding some function that estimates the position of Te from the samples contained in the interval between two consecutive R peaks. In practice, due to heart rate variability, RR intervals contain a variable number of samples. Then, this general form of stating the problem is not practical since it involves to find a function with variable dimensions. To avoid this problem, it is possible to use a fixed-size window, i.e., the domain of such function has dimension n (n fixed), see Figure 1.

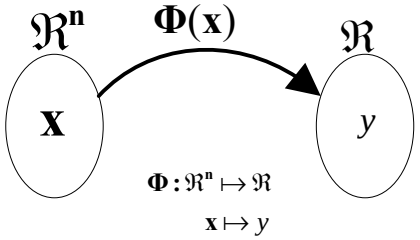

Figure1. Mapping function $\Phi(\mathbf{x})$, the input signal samples ($\mathbf{x}$) determines the distance of Te (y) to a reference point.

Now, the problem is to find a mapping $\Phi(\mathbf{x})$ function between $\mathbf{x} \in \Re^{\mathbf{n}}$ and $y \in \Re$ where y is the location of the Te starting from a reference point.

This study focuses on Multilayer Perceptron (MLP) neural network architectures to estimate $\Phi(\mathbf{x})$ using Bayesian regularization for training. The dataset used was the QT Database (QTDB) [8]. The QTDB was designed for evaluating the performance of algorithms for event detection on ECG. It consists of short segments (15 min) extracted from 105 Holter recordings, each with two channels. All records have a sampling frequency of 250 Hz. 3542 Te were annotated by one cardiologist. Another cardiologist has annotated 402 Te in 11 recordings.

2.1. Pre-processing and segmentation

The pre-processing stage uses a fourth order band-pass Butterworth filter to deal with both baseline wandering and high frequency noises. The cut-off frequencies were 0.5 Hz and 50 Hz for high-pass and low-pass respectively.

The R-peak detection algorithm used is based on parabolic fitting [9]. The segmentation is as follows: for each annotated beat, a 100 samples vector (400 ms) is extracted from a reference point at R + 200 ms (R is the R-peak location of the current ECG beat), see Figure 2.

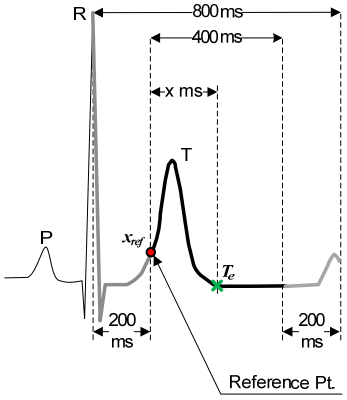

Figure 2. Window selection for segmentation.

The 200 ms offset intends to skip the samples from the QRS complex. Then, mostly samples from the current T wave will be considered. This process is expressed as:

$$\mathbf{x_i} = s[R_i + 200 : R_i + 600] \tag{1}$$

Where s corresponds to the signal and R_i represents the time location of the R-peak for the current beat, $\mathbf{x_i}$ is the 100 samples vector for each beat.

The target output (y_i) for each vector is:

$$y_i = \frac{Te_i - x_{ref}}{400} = \frac{Te_i - R_i - 200}{400} \tag{2}$$

where Te_i, corresponds to the Te annotated by the cardiologist. The values of y_i were normalized from 0 to 1, via a division by 400 ms.

2.2. Methods for dimensional reduction

The number of components of each $\mathbf{x_i}$ is 100, this dimension is still large to be used as input to the regression algorithm (neural network), therefore, three different dimension reduction (DR) techniques are used: resampling (RES), Discrete Cosine Transform (DCT) and Principal Component Analysis (PCA).

The resampling (RES) operation takes a $\mathbf{x_i}$ vector and applies it to a sub-sampler system.The sub-sampler consists of two functional blocks, an anti-aliasing filter ($H(z)$) and a decimator defined as (see Figure 3).

$$x_d[k] = x[kD],\ D \in \mathbf{N}, D \neq 0 \tag{3}$$

where D is the decimation factor. This paper uses D = 6 because 100 samples in the input reduce to 16 samples at the output (the number of input neurons, see Figure 4). The anti-aliasing filter is a low-pass FIR designed with the LMS algorithm using a Kaiser window.

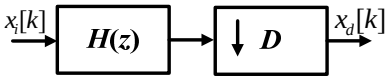

Figure 3. Sub-sampler system structure.

The DCT is the discrete form of the Cosine Fourier Transform (CFT), and it is written as.

$$y(k) = a(k)\sum_{n=0}^{N-1} x_n \cos\left(\frac{\pi n k}{N-1}\right) \quad n = 0,\ldots,N-1$$
$$a(k) = \begin{cases} \frac{1}{\sqrt{N}}; & k = 0 \\ \sqrt{\frac{2}{N}}; & 1 \le k \le N-1 \end{cases} \tag{4}$$

PCA takes the projections of a vector over the subspace generated by the M eigenvectors associated to the M largest eigenvalues from the covariance matrix of the data, defined as.

$$\mathbf{C} = \frac{1}{N}\sum_{j=1}^{N} \mathbf{x}_j \mathbf{x}_j^{\mathbf{T}} \tag{5}$$

Next, the following eigenvalue problem needs to be solved:

$$\lambda \mathbf{v} = \mathbf{C}\mathbf{v} \qquad \lambda \geq 0 \wedge \mathbf{v} \in \Re^{\mathbf{n}} \setminus \{\mathbf{0}\} \tag{6}$$

Projecting the input over the subspace generated by the M vectors ($M<N$) associated to the greatest eigenvalues results in a dimensional reduction of the data.

2.3. Multilayer Perceptron and Bayesian Regulation

The used MLP networks have three layers: input, hidden and output. For each technique of dimensionality reduction, a set of MLP networks were trained varying the number of input neurons from 1 to 16, and the number of hidden neurons from 1 to 32, resulting in 512 architectures per method, see Figure 4.

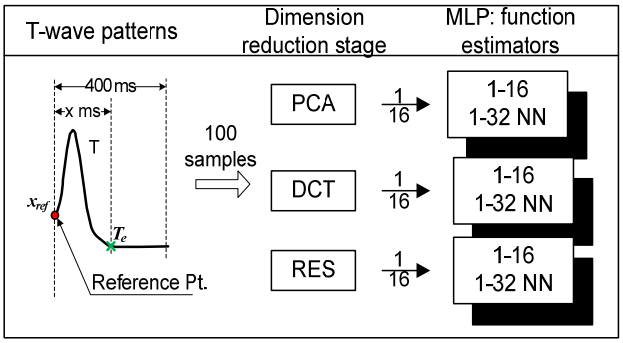

Figure 4. General diagram for MLP-based Te detectors

The activation functions for the hidden and output layers are the hyperbolic tangent (tanh) and linear function, respectively. The training function is Backpropagation-Bayesian Regulation. The training error function used is:

$$E = \frac{1}{2}\sum_i \left(\Phi(\mathbf{x}_i) - y_i\right)^2 + \frac{1}{2}\sum_i \omega_i^2 \tag{7}$$

where $\Phi(\mathbf{x})$, is the output of the neural network given the pattern $\mathbf{x_i}$, and ω_i represents all the weights and biases of the neural network. The second term in the expression (7) is the weight decay regularizer.

To prevent outliers in the training, the whole data set was filtered using the following constraint: given a pair $P_i = (\mathbf{x_i}, y_i)$, P_i will be eligible as a training sample if and only if y_i belongs to the range [-0.5, 1.5] i.e. the Te point is inside the 800 ms window. Using this criterion, only 106 beats (~1.5%) were excluded.

A new training subset is randomly generated from the eligible dataset every time the number of input neurons (or components at the output of the DR stage) changes. 30% (2093 pairs) of the eligible dataset was used as training set.

The performance measure used to evaluate the generalization of the network was the precision (standard deviation of the error in milliseconds) over the validation set:

$$\sigma = \sqrt{\frac{1}{V-1}\sum_{i=1}^{V}(e_i - \bar{e})^2} \tag{8}$$

where V is the number of patterns in the validation set, i.e. V= 4885.

3. Results and discussion

The precision in validation for each dimensional reduction method is distributed according to the following ranges (all values in milliseconds): σ(PCA) = [35.22, 70.77]; σ(DCT) = [34.94, 117.63] and σ(RES) = [33.43, 68.37]. Figure 5 shows the distribution of the values of precision in 10 ms intervals.

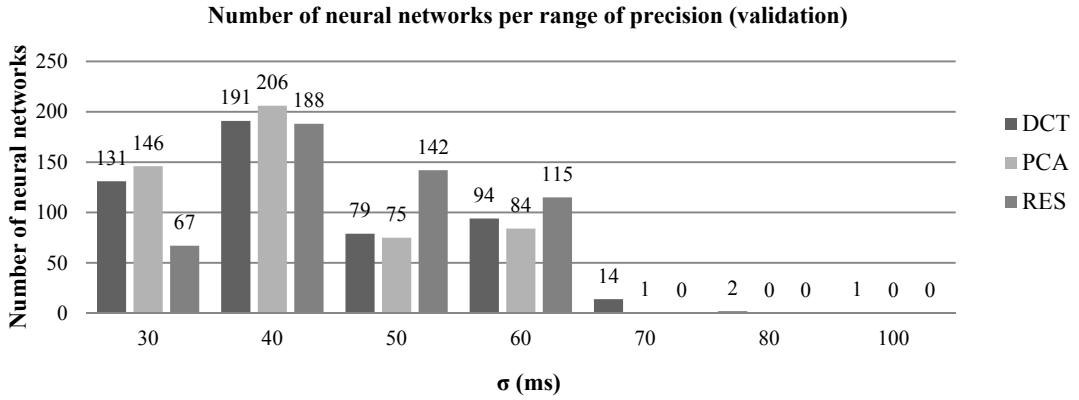

Figure 5. Distribution of the precision in validation for each DR method

Using as reference the 30-40 ms interval (344 neural networks with the best results), the approaches that use the DCT and PCA methods are the biggest group (~80%) on this interval. Conversely, RES represents only 20% of the total. Hence, RES approach produces fewer architectures with acceptable performance (σ <40 ms). This is because the effectiveness of the RES method heavily depends on preserving a high number of components (12 to 16). Also, the RES method shows the worst overall mean value of precision (51.17 ± 9.22 ms). Both approaches, PCA and DCT have better mean precision than RES, for DCT the mean value of precision is 45.65 ± 14.72 ms while for PCA the mean precision is 46.17 ± 9.48 ms.

In conclusion, the RES approach requires the use of a greater number of features, making it less effective in reducing the size of the network in comparison with the other two methods. However, this does not mean that the RES method cannot produce good results. Table 1 shows the evaluation of the best architectures for each approach using the criterion "best beat per cardiac cycle", Martínez *et al.* [2].

Table 1. Best results for each dimensional reduction method

Method	Neural Network	Error: m ± std (ms)
DCT	16-31-1	-0.06 ± 15.45
PCA	16-29-1	-0.50 ± 15.34
RES	16-19-1	-0.12 ± 15.06

The results of the Te detection algorithms reported in the literature are shown in Table 2. The proposed method allows building MLP-based Te detectors with performances comparable to those of the state of the art.

Table 2. Algorithms for detecting the Te on the ECG

Detector	Error: m ± std (ms)
Madeiro *et al.* [7]	2.80 ± 15.30
This work (best precision)	**-0.12 ± 15.06**
Vázquez *et al.* [4]	1.98 ± 16.90
Lin *et al.* [6]	4.30 ± 20.80
A. Martínez *et al*. [10]	5.80 ± 22.70
Ghaffari *et al.* [5]	0.80 ± 10.70
Zhang *et al.* [3]	0.31 ± 17.43
This work (best accuracy)	**-0.06 ± 15.45**
Martínez *et al.* [2]	-1.6 ± 18.10
Vila *et al.* [1]	0.80 ± 30.30

The accuracy (mean error value) of the three MLP-based Te detectors is comparable to the accuracy of Zhang's method (the best). Meanwhile, the precision is in the range of the method of Madeiro *et al.* [7], the second best one after Ghaffari's method.

Acknowledgements

This work has been supported by the Belgian Development Cooperation through VLIR-UOS (Flemish Interuniversity Council-University Cooperation for Development) in the context of the Institutional University Cooperation programme with Universidad de Oriente.

References

[1] Vila JA, Gang Y, Presedo JMR, Delgado MF, Barro S, Malik M. A new approach for TU complex characterization. IEEE Trans Biomed Eng. 2000;47(6):764–72.

[2] Martinez JP, Almeida R, Olmos S, Rocha AP, Laguna P. A Wavelet-Based ECG Delineator: Evaluation on Standard Databases. IEEE Trans Biomed Eng. 2004;51:570-81.

[3] Zhang Q, Manriquez AI, Médigue C, Papelier Y, Sorine M. An algorithm for robust and efficient location of T-wave ends in electrocardiograms. IEEE TransBiomedEng. 2006;53(12):2544–52.

[4] Vázquez S. CR, Neto JE, Reyes EJM, Klautau A, Oliveira RCL. New approach for T-wave end detection on electrocardiogram: performance in noisy conditions. Biomed Eng Online. 2011;10(77):1-11.

[5] Ghaffari A, Homaeinezhad MR, Akraminia M, Atarod M, Daevaeiha M. A robust wavelet-based multi-lead electrocardiogram delineation algorithm. Med Eng Phys. 2009;31:1219–27.

[6] Lin C, Mailhes C, Tourneret J-Y. P- and T-Wave Delineation in ECG Signals Using a Bayesian Approach and a Partially Collapsed Gibbs Sampler. IEEE Transactions on Biomedical Engineering. 2010;57(12):2840-9.

[7] Madeiro JPV, Nicolson WB, Cortez PC, Marques JAL, Vázquez S. CR, Elangovan N, et al. New approach for T-wave peak detection and T-wave end location in 12-lead paced ECG signals based on a mathematical model. Medical Engineering & Physics. 2013;35:1105-15.

[8] Laguna P, Mark R, Goldberger A, Moody GB. A database for evaluation of algorithms for measurement of QT and other waveform intervals in the ECG. ComputCardiol. 1997;24:295-8.

[9] Manriquez AI, Zhang Q. An algorithm for QRS onset and offset detection in single lead electrocardiogram records. Proceedings of the 29th Annual International Conference of the IEEE EMBS; Lyon, France: IEEE; 2007. p. 541-4.

[10] Martínez A, Alcaraz R, Rieta JJ. Application of the phasor transform for automatic delineation of single-lead ECG fiducial points. Physiol Meas. 2010;31:1467-85.

Address for correspondence.

Alexander Alexeis Suárez León
Departamento de Ingeniería Biomédica, Facultad de Ingeniería Eléctrica, Universidad de Oriente. Ave. Américas y Casero. 90400, Santiago de Cuba, Cuba.
aasl@fie.uo.edu.cu